AFRL-ML-WP-TR-2004-4281

NONDESTRUCTIVE EVALUATION (NDE) TECHNOLOGY INITIATIVE PROGRAM (NTIP)
Delivery Order 0038: NDE Sensory Monitoring System for Aircraft Structure

M. Sundaresan, G. Grandhi, S. Uppaluri, and J. Kermerling

North Carolina A&T State University
Department of Mechanical and Chemical Engineering
1601 East Market Street
Greensboro, NC 27411

JULY 2003

Final Report for 01 October 2002 – 31 May 2003

STINFO FINAL REPORT

MATERIALS AND MANUFACTURING DIRECTORATE
AIR FORCE RESEARCH LABORATORY
AIR FORCE MATERIEL COMMAND
WRIGHT-PATTERSON AIR FORCE BASE, OH 45433-7750

NOTICE

USING GOVERNMENT DRAWINGS, SPECIFICATIONS, OR OTHER DATA INCLUDED IN THIS DOCUMENT FOR ANY PURPOSE OTHER THAN GOVERNMENT PROCUREMENT DOES NOT IN ANY WAY OBLIGATE THE U.S. GOVERNMENT. THE FACT THAT THE GOVERNMENT FORMULATED OR SUPPLIED THE DRAWINGS, SPECIFICATIONS, OR OTHER DATA DOES NOT LICENSE THE HOLDER OR ANY OTHER PERSON OR CORPORATION; OR CONVEY ANY RIGHTS OR PERMISSION TO MANUFACTURE, USE, OR SELL ANY PATENTED INVENTION THAT MAY RELATE TO THEM.

THIS REPORT HAS BEEN REVIEWED BY THE OFFICE OF PUBLIC AFFAIRS (ASC/PA) AND IS RELEASABLE TO THE NATIONAL TECHNICAL INFORMATION SERVICE (NTIS). AT NTIS, IT WILL BE AVAILABLE TO THE GENERAL PUBLIC, INCLUDING FOREIGN NATIONALS.

THIS TECHNICAL REPORT HAS BEEN REVIEWED AND IS APPROVED FOR PUBLICATION.

/s/   /s/
_____   _____
JUAN G. CALZADA, Project Engineer   JAMES C. MALAS, Chief
Nondestructive Evaluations Branch   Nondestructive Evaluations Branch
Metals, Ceramics & NDE Division   Metals, Ceramics & NDE Division

/s/
_____
GERALD J. PETRAK, Assistant Chief
Metals, Ceramics & NDE Division
Materials & Manufacturing Directorate

DO NOT RETURN COPIES OF THIS REPORT UNLESS CONTRACTUAL OBLIGATIONS OR NOTICE ON A SPECIFIC DOCUMENT REQUIRES ITS RETURN.

REPORT DOCUMENTATION PAGE

The public reporting burden for this collection of information is estimated to average 1 hour per response, including the time for reviewing instructions, searching existing data sources, searching existing data sources, gathering and maintaining the data needed, and completing and reviewing the collection of information. Send comments regarding this burden estimate or any other aspect of this collection of information, including suggestions for reducing this burden, to Department of Defense, Washington Headquarters Services, Directorate for Information Operations and Reports (0704-0188), 1215 Jefferson Davis Highway, Suite 1204, Arlington, VA 22202-4302. Respondents should be aware that notwithstanding any other provision of law, no person shall be subject to any penalty for failing to comply with a collection of information if it does not display a currently valid OMB control number. **PLEASE DO NOT RETURN YOUR FORM TO THE ABOVE ADDRESS.**

1. REPORT DATE *(DD-MM-YY)*	2. REPORT TYPE	3. DATES COVERED *(From - To)*
July 2003	Final	10/01/2002 – 05/31/2003

4. TITLE AND SUBTITLE	5a. CONTRACT NUMBER
NONDESTRUCTIVE EVALUATION (NDE) TECHNOLOGY INITIATIVE PROGRAM (NTIP) Delivery Order 0038: NDE Sensory Monitoring System for Aircraft Structure	F33615-97-D-5271-0038

5b. GRANT NUMBER

5c. PROGRAM ELEMENT NUMBER
62102F

6. AUTHOR(S)	5d. PROJECT NUMBER
M. Sundaresan, G. Grandhi, S. Uppaluri, and J. Kermerling	4349

5e. TASK NUMBER
40

5f. WORK UNIT NUMBER
01

7. PERFORMING ORGANIZATION NAME(S) AND ADDRESS(ES)	8. PERFORMING ORGANIZATION REPORT NUMBER
North Carolina A&T State University Department of Mechanical and Chemical Engineering 1601 East Market Street Greensboro, NC 27411	

9. SPONSORING/MONITORING AGENCY NAME(S) AND ADDRESS(ES)	10. SPONSORING/MONITORING AGENCY ACRONYM(S)
Materials and Manufacturing Directorate Air Force Research Laboratory Air Force Materiel Command Wright-Patterson AFB, OH 45433-7750	AFRL/MLLP
	11. SPONSORING/MONITORING AGENCY REPORT NUMBER(S) AFRL-ML-WP-TR-2004-4281

12. DISTRIBUTION/AVAILABILITY STATEMENT
Approved for public release; release is unlimited.

13. SUPPLEMENTARY NOTES
Report contains color.

14. ABSTRACT

The concept of a biomimetic sensor system design that can be embedded in aircraft structure is explored in this project. Signal processing techniques for quantifying the sensor responses are studied. In particular wavelet analysis is used to extract the time frequency information about the acoustic emission signals and to separate the Lamb wave modes. The continuous sensor used in this biomimetic sensor system was used to monitor fatigue crack extensions in a glass epoxy composite panel. The sensor was found to be sufficiently sensitive to detect fatigue crack growth rates of the order of 4 x 10^{-6} inch/cycle. The waveforms from the mode I type crack growth had some differences. Based on these differences, nine different AE signal types were identified and their relative frequency components were examined. Further, continuous sensor with its distributed sensing nodes was shown to be superior to traditional single node acoustic emission sensors particularly for monitoring highly attenuative structures such as composite panels and large regions. In addition, an algorithm for locating the source of acoustic emission signals in a two-dimensional plane from the signal from a single channel continuous sensor was developed and verified through numerical simulations. As a final part of this effort, an emulator of the embeddable local processor chip that is a key element in the biomimetic sensor system was developed.

15. SUBJECT TERMS
biomimetic sensor, aircraft structures, wavelet analysis, fatigue crack growth

16. SECURITY CLASSIFICATION OF:			17. LIMITATION OF ABSTRACT:	18. NUMBER OF PAGES	19a. NAME OF RESPONSIBLE PERSON (Monitor)
a. REPORT Unclassified	**b. ABSTRACT** Unclassified	**c. THIS PAGE** Unclassified	SAR	42	Juan Calzada 19b. TELEPHONE NUMBER *(Include Area Code)* (937) 255-9761

TABLE OF CONTENTS

1.0 Introduction

With the aging fleet of the civilian and military aircrafts, there is an increasing need for the development of Structural Health Monitoring (SHM) systems. An effective SHM system can increase the reliability and reduce the operational cost of the fleet. Frequently, the damage to structures is diffused and/or widely distributed, and sometimes can be inaccessible to conventional NDE techniques. This is often the case for fatigue damage to composite structures and multi-site fatigue damage in aging aluminum aircraft structures. Currently, most of the NDE of helicopters and aircrafts is being performed using manual techniques. These inspections are labor intensive and involves significant vehicle downtime. It is also difficult to reliably document the NDE data. Periodic large area surveys on aging air vehicles can detect widespread fatigue damage, but this is very expensive and time consuming. Structural health monitoring using acoustic emission technique can effectively compliment the depot-based NDE and significantly enhance the reliability of aircraft structures. However, for such an acoustic emission based SHM technique to be implemented in practice, some of the major limitations of the traditional acoustic emission technique have to be overcome. While the AE technique has excellent sensitivity to detect incipient damage growth in structural members, it is not widely used for structural health monitoring. The major limitation of AE technique is that a prohibitively large number of AE sensors and instrumentation channels are required for monitoring the large number of possible damage sites on a complex structure such as aircraft. An AE sensor that can cover a wide area with complex acoustical paths, while

retaining the single channel attribute can drastically simplify AE instrumentation and form a key technology for practical structural health monitoring. A distributed sensor illustrated in figure 1, and described under section 2, was recently proposed as a means of achieving this advancement. Such distributed sensors can reduce the complexity, cost, and weight of the AE instrumentation. The sensor system can be embedded in composite structures and bonded on the surface of metallic structures. It can monitor the structure during flight and provide real-time assessment of crack growth.
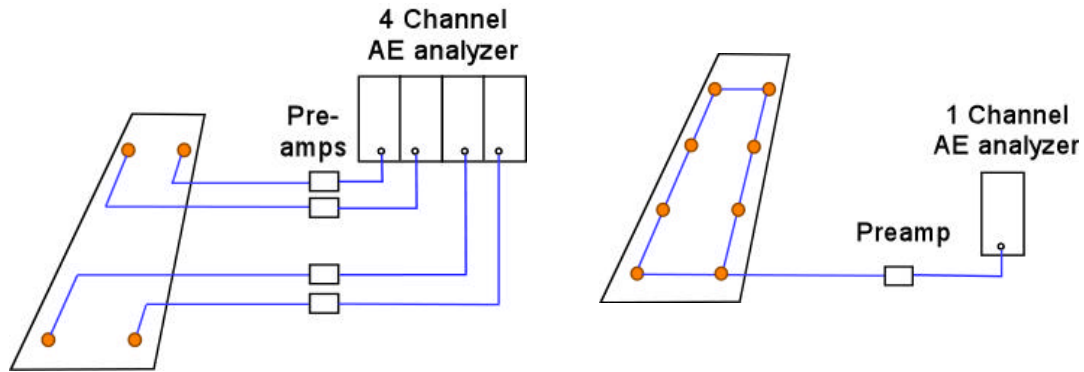
Figure 1 (a) Traditional acoustic emission instrumentation and (b) Instrumentation that uses continuous sensor

2.0 Continuous Sensor and the Unit Cell of the Structural Health Monitoring System

A continuous sensor is formed by combining multiple sensors nodes in a series arrangement that combines the sensor responses into single electrical output signal. Figure 1 illustrates the formation of continuous sensor and compares the instrumentation that uses continuous sensor with that of traditional AE sensor. Continuous sensor can enable provide a significant increase in the sensitivity with a simultaneously reducing the number of instrumentation channels. The performance of continuous sensor has been

evaluated using simulated AE signals as well as real flaw growth in metallic and composite materials [1-3].

In addition to this simplification, a unit cell shown in figure 2(b) was designed to further enhance the adaptability of the sensor system for weight critical applications such as those in aircraft or space applications. An embeddable local processor that is placed in the midst of the sensor nodes, can perform both the analog signal conditioning including amplification and filtering, as well as the digital signal processing to extract the main attributes of the detected acoustic emission signal was proposed [5]. The signal processing will reduce the high volume input data into a compact set of AE parameters only about ten bytes long for each AE event. The micro miniaturization of electronics makes it possible to fabricate such an embeddable processor using current technology. The illustration shown in Figure 2(b) includes an array of three such unit cells, with each unit cell containing 9 sensor nodes and a local processor. These local processors will also communicate with a central processor over a digital bus and periodically upload processed information to the central computer. As illustrated in figure 2, the unit cells retains the simplicity and scalability of the biological nerve cells, and hence is attractive for building health monitoring system for large and complex structures. The fist generation of local processors will have the most basic functions required for measuring the damage growth in the region covered by the unit cell. Further refinements will be introduced at a later stage.
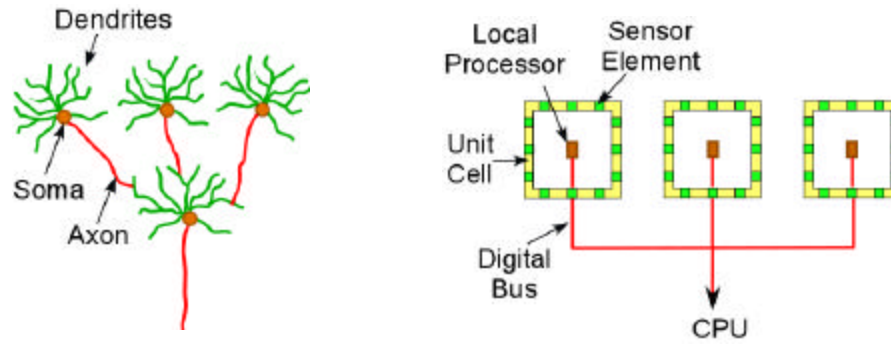
Figure 2. Unit cells of the proposed structural health monitoring system. (a) Simplified illustration of biological nervous system, (b) Unit cells with autonomous sensing, signal processing, and communication capability that are similar to individual nerve cells.

3.0 Scope of the current work

(a)   The concept of continuous sensor is evaluated using a composite panel with fatigue cracks. The performance of the continuous crack is compared with that of conventional acoustic emission sensor. New signal processing technique to extract the time-frequency information about the individual acoustic emission signals is investigated. In addition an algorithm for location of the AE source occurring anywhere in a plane is developed.

(b)   An emulator for the local processor that will be incorporated into the local processor was developed.

4.0 Monitoring of simulated AE signals in an aluminum plate

The current investigation was begun with the characterization of simulated AE signals in aluminum and composite specimens. The simulated AE signals were introduced using a 0.125" active element AE sensor as a pulser. This pulser was excited using a 400 V, 0.2

4

microsecond wide square wave pulse. The longitudinal wave that is introduced by the pulser normal to the plate surface excites Lamb waves in the plates that propagate along the plane of the plate and has been found to be similar to AE signals generated by incremental crack growth. The simulated AE signals are employed in the present study to (a) understand how AE waves propagate through different materials, (b) evaluate the working of sensors, (c) get an approximate measure of the attenuation in the structure,
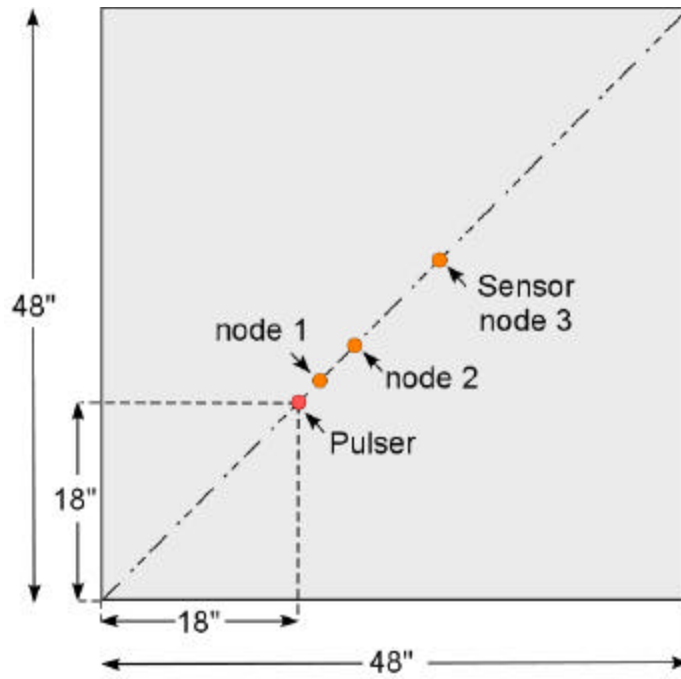
Figure 3. Simulation of AE signals and continuous sensor on an aluminum plate

and (d) verify the wavelet techniques. Three 0.25" diameter 5MHz ultrasonic sensors were used as the nodes of the continuous sensor. The highly damped ultrasonic sensors were chosen for their superior wide band sensing capability, compact size, and their ability to reproduce the AE signals reasonably accurately. Traditional resonant frequency

AE sensors cannot reproduce the AE waveforms faithfully. The signals from these sensors were amplified by 34 dB, and digitized using a LeCroy digital oscilloscope.

Wavelet Transforms are relatively new technique, which allows determination of the frequency spectrum as a function of time using wavelets as basis function. These transforms have been successfully utilized for analyzing various dynamic signals. Morlet wavelet is one of the different families of wavelets and it has been successfully applied to signal processing. The Morlet wavelet analysis applied to the present waveforms clearly shows the different frequencies present in the signal and their relative amplitudes.

The first set of signal acquisition and analysis was performed on simulated AE signal that propagated on a relatively large aluminum plate. A 48" x 48" square plate with a thickness of 0.25" shown in figure 3 was chosen for this study. The pulser as well as the sensors were located along a diameter of the plate to delay reflected stress waves from arriving at the sensors. The relatively short source to sensor distances was necessitated by the relatively small size of the aluminum plate and the desire to separate the main pulse from the reflections from the edges.
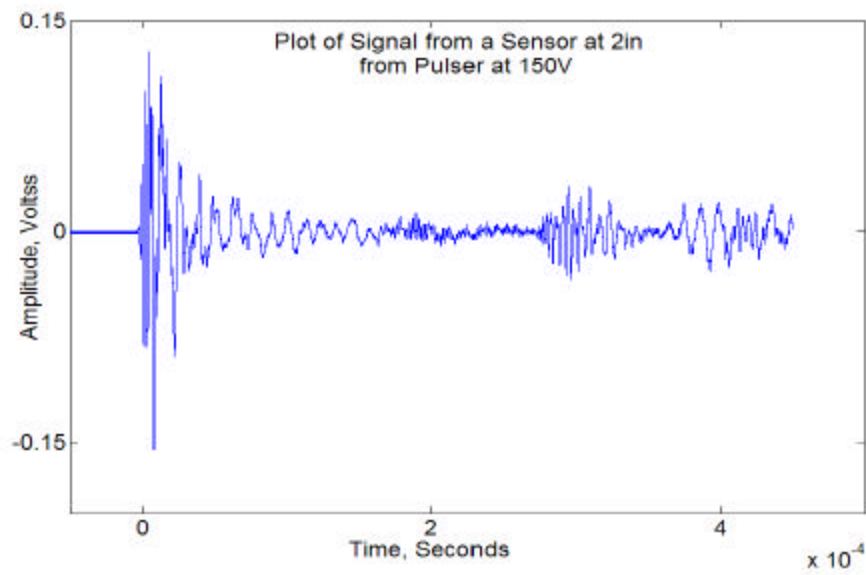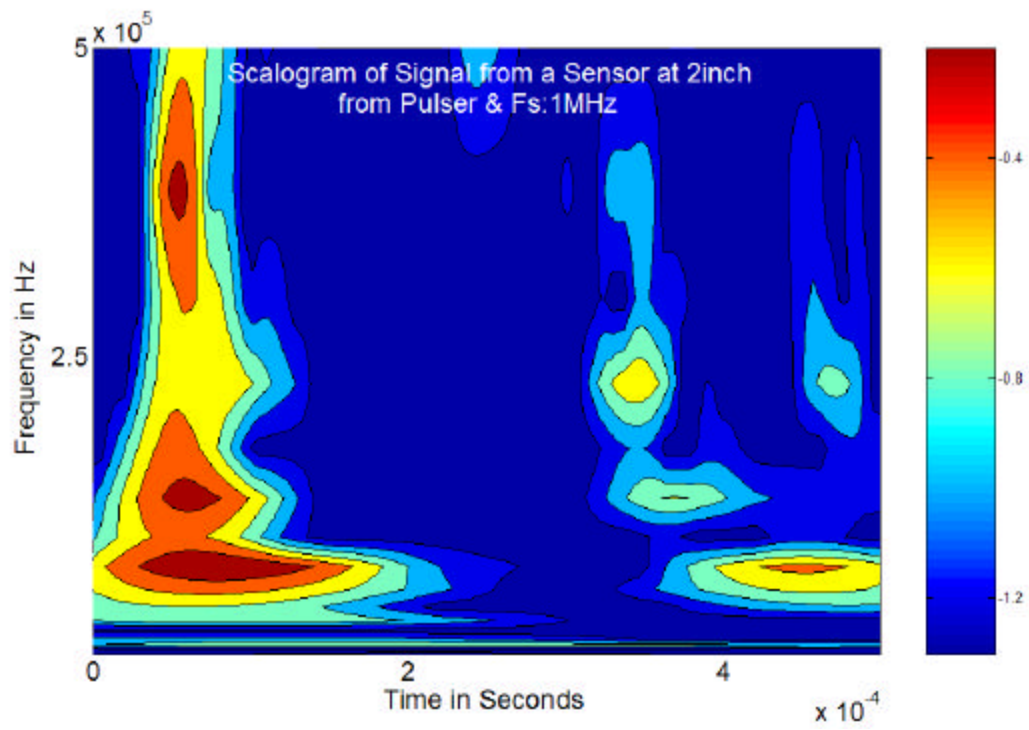
Figure 5. The Morlet wavelet map of signal from sensor node 1 on the aluminum plate
and the waveform of the signal.

The waveform corresponding to the simulated AE signal from sensor node 1 is shown in figure 4. Morlet wavelet analysis of this waveform is also shown in figure 4. This figure indicates the presence of several distinct modes traveling at different velocities. Frequencies up to 0.5 MHz were seen. The first group of contours in the wavelet map in figure 4 corresponds to the direct pulse i.e., the stress wave reaching the sensor 1 along the shortest path from the source, and in this group of contours the temporal separation of the different modes reaching the sensor 1 is minimum. The second group of contours in the wavelet map corresponding to pulses reflected from the plate edges, possibly overlapping of several reflections. In this group of contours, the dispersion of the stress waves is easily seen. The duration of the waveform shown in the figure 4 is 0.5 ms and this included one set of reflected contours. In a longer waveform, obviously, more reflections would be included and hence the AE signal would appear more complex. The waveforms and the corresponding wavelet maps for sensors 2 and 3 are shown in figures 5 and 6.
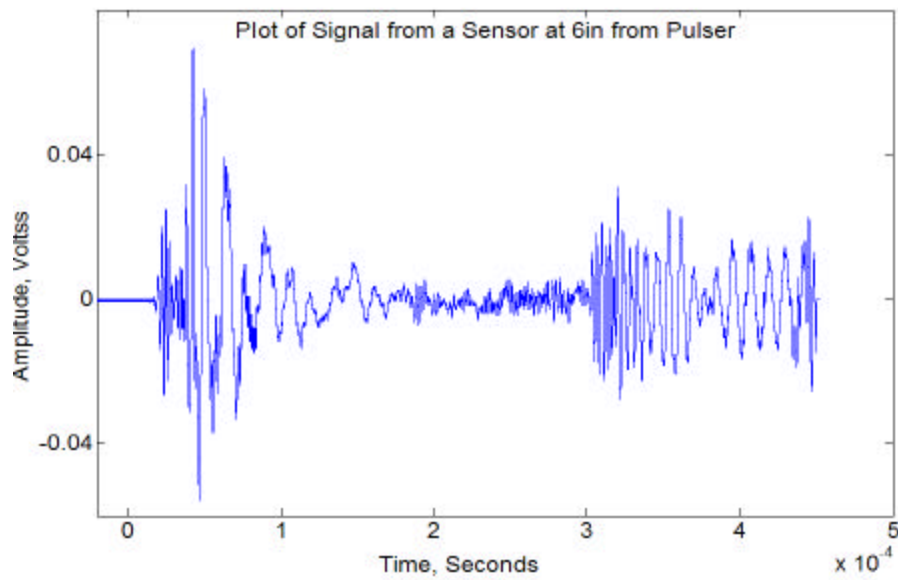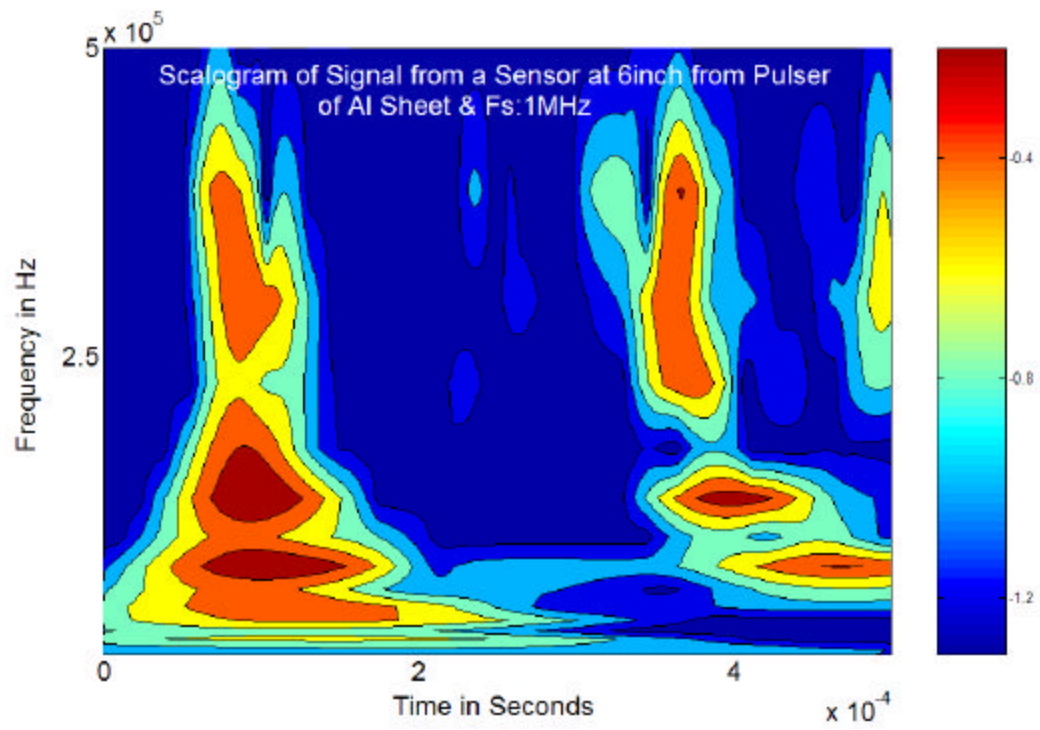
Figure 6. The Morlet wavelet map of signal from sensor node 2 on the aluminum plate
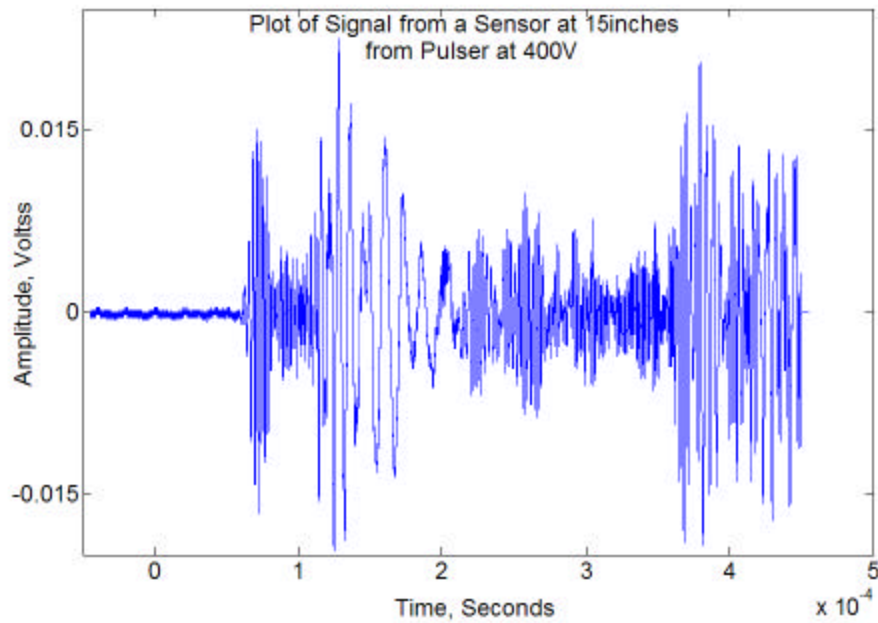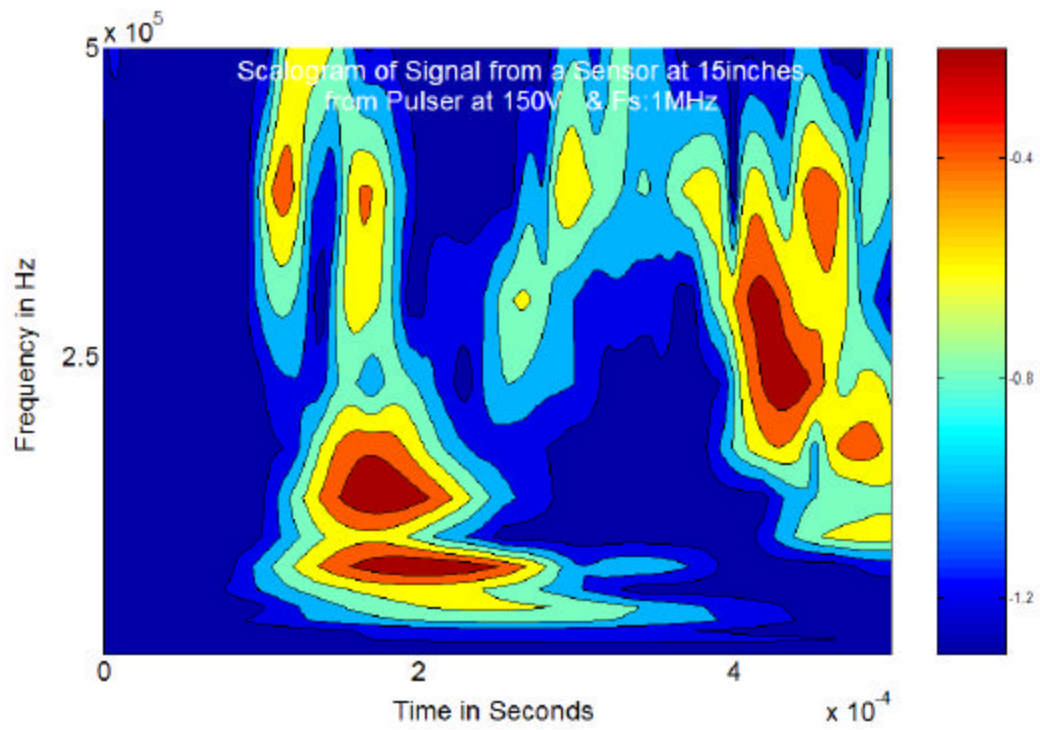and the waveform of the signal.

Figure 7. The Morlet wavelet map of signal from sensor node 2 on the aluminum plate and the waveform of the signal.
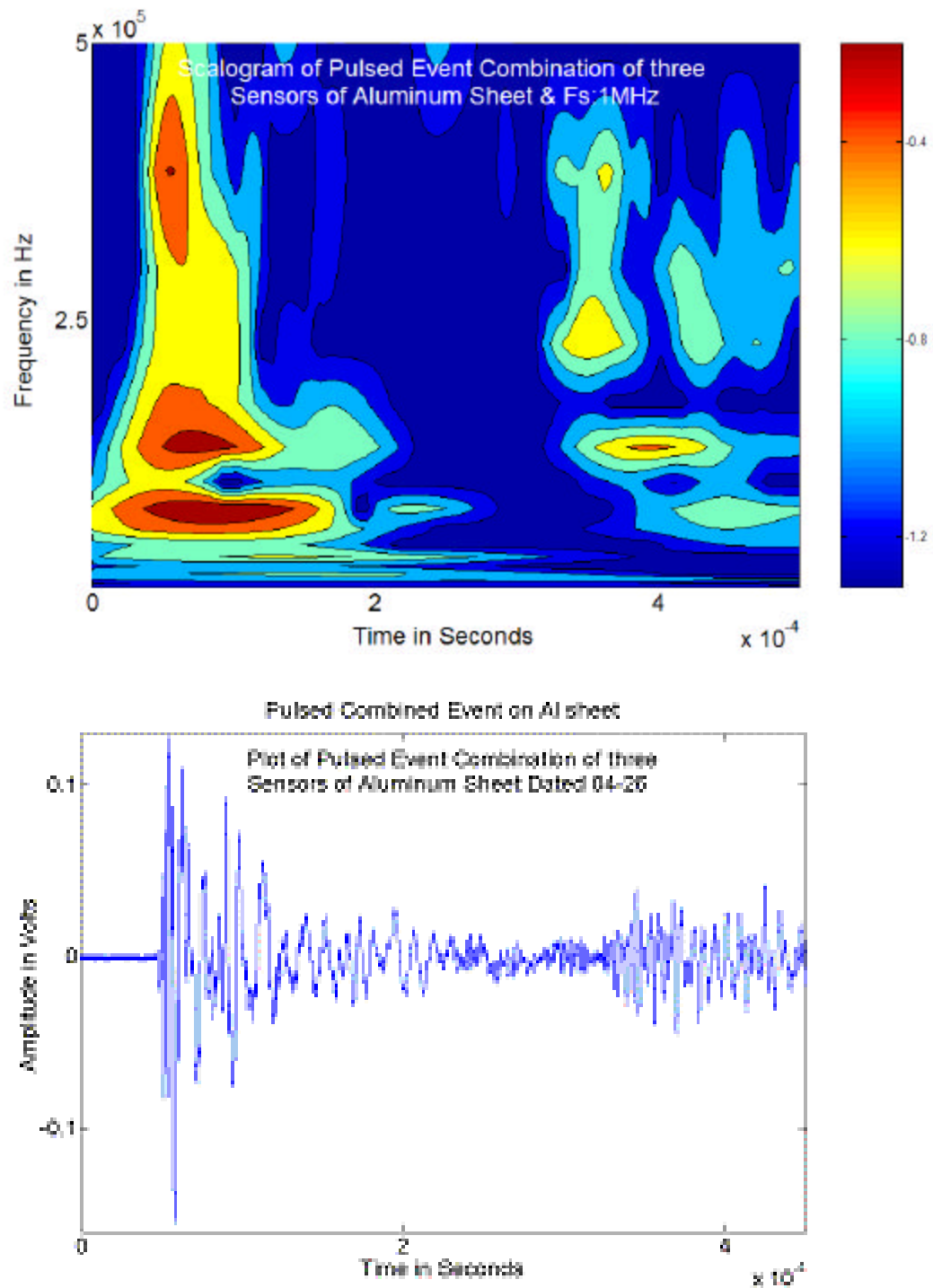
Figure 7. The Morlet wavelet map of combined signal from sensor nodes 1 to 3 on the aluminum plate and the waveform of the signal.

The differences in the received waveforms at these three source to sensor distances are quite significant. The presence of the different Lamb wave modes and their differing velocities are seen in the wavelet maps in figure 5 and 6 to a greater extent compared to the ones seen in figure 4 corresponding to a source to sensor distance of 2". Even in aluminum plate that has a relatively small level of attenuation, the peak-to-peak amplitudes dropped significantly as the stress wave traveled the relatively short distances. For the three source to sensor distances of 2", 6", and 15" signal amplitudes were 0.3 V, 0.15 V, and 0.04 V, respectively. Dispersion is one of the contributing factors for this change in signal amplitude. In addition, the waveforms corresponding to sensors 2 and 3 are more complex compared to the first sensor because sensors 2 and 3 captured more reflected signals compared to first one.

The waveform seen in figure 7 is obtained simply by adding the waveforms corresponding to sensors at 2", 6", and 15" shown in the earlier figures. This would approximately the waveform obtained by a continuous sensor with three nodes located at these three distances. The wavelet map corresponding to this waveform is also shown in figure 7. As expected this waveform is dominated by the first hit sensor node, which in this case is sensor1, and retains the high signal to noise ratio, relatively small dispersion, less dominant reflections from the reflections, and hence greater clarity in the signal for analysis purposes. This would be true irrespective of which sensor node is hit first. The configuration of this hypothetical continuous sensor was chosen for illustration purposes only and is not optimized. As shown in section on planar location of AE source, under certain circumstances it is possible to locate the source of the AE signal, for such

capability the sensor nodes should be suitably locate. An inspection of the wavelet maps and waveforms clearly indicate the value of using the wavelet analysis. Wavelet analysis clearly indicates the different Lamb wave modes traveling at different velocities and using wavelet maps is possible to separate initial pulse from reflected pulses.

5.0 Simulation test on Composite Panel

The performance of the continuous sensor was evaluated by monitoring the simulated acoustic emission signals as well as acoustic emission signals from incremental crack growth during fatigue loading on a composite panel. The composite panel used in this study was 16 inches long, 6 inches wide, and 0.125-inch thick and was prepared from a woven glass fabric epoxy laminate. This panel had a 0.5-inch diameter at the center. Two slits approximately 0.125" long were cut on either side of the circular hole using a fine saw as shown in figure 8. A loading fixture for this acoustic emission study was designed and built, and the assembly of the plate in the fixture is shown in figure 8. Since the attenuation of emissions in composite panel is much more compared to aluminum specimens, the proposed continuous sensory system can play a vital role in capturing the signals before the signal gets smaller than the prevailing noise level due to attenuation. The composite panel was subjected to fatigue load until fatigue cracks approximately 0.04-inch fatigue cracks appeared at the ends of both of the horizontal slits.

After pre-cracking the panel, a continuous sensor with six nodes was bonded at the locations shown in the figure and was connected in series. One of the six nodes of the continuous sensor was placed at the proximity of each of the two known fatigue crack

locations. The objective of these experiments to evaluate the continuous sensor for detecting fatigue cracks in composite panels. AE source location was not planned during these tests. Copper foils were used for shielding the continuous sensor from RF noise. The panel was also instrumented with traditional single node sensors, which were the 5 MHz sensors, used in the previous simulations. The locations of the continuous sensor nodes as well as the single nodded sensors are shown in figure 8. The numbers adjacent to the sensors in this figure are the vertical distances from the horizontal centerline of the panel. To avoid cluttering, only the locations of continuous sensor nodes are shown, but the sketch is drawn to scale. The single node sensor C_3 is at 2 inches from the right edge and 1.375 inch along the vertical direction from notch. C_4 was located at a diametrically opposite position. The single node sensors C_1 and C_2 were used as guard sensors during the initial portion of the fatigue loading to ascertain that the signals detected by the continuous sensor were not due to noise from the testing machine or fretting noise from the gripping plates.

The pulser was used to simulate AE signals at two different positions. First it was placed at the location P_1, which was close to one of the fatigue cracks, to inject simulated AE pulses and the signals detected from the continuous sensor as well as the single node sensors C_3 and C_4 were recorded. Then the pulser was moved to location P_2 close to the gripping plates and the procedure was repeated.
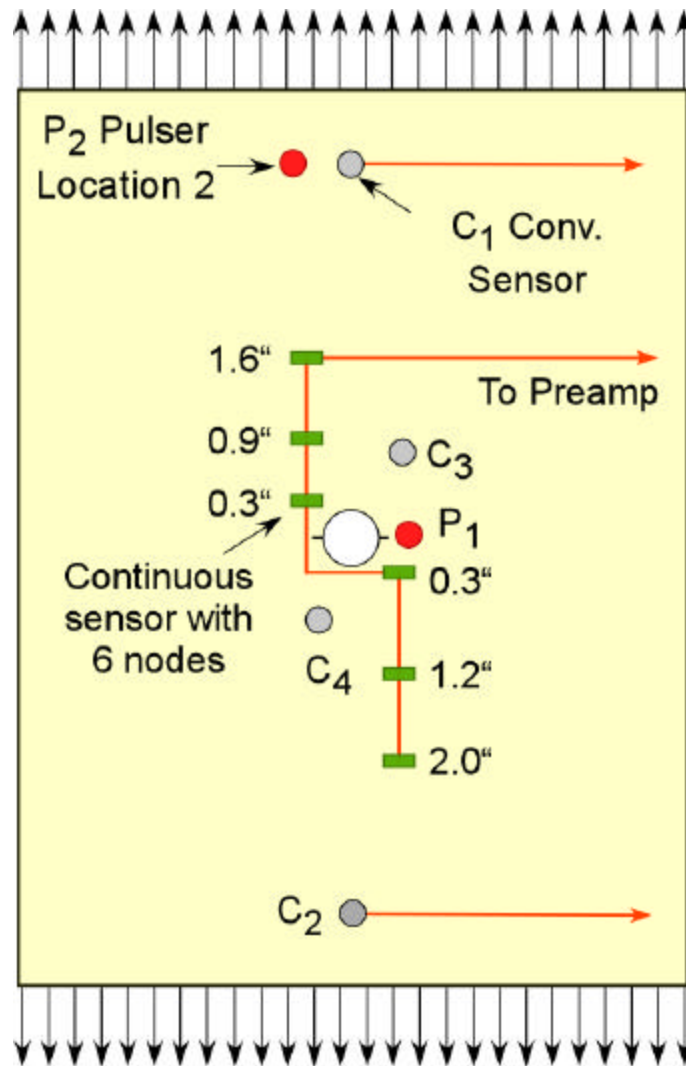
Figure 8: the arrangement of sensor on composite panel

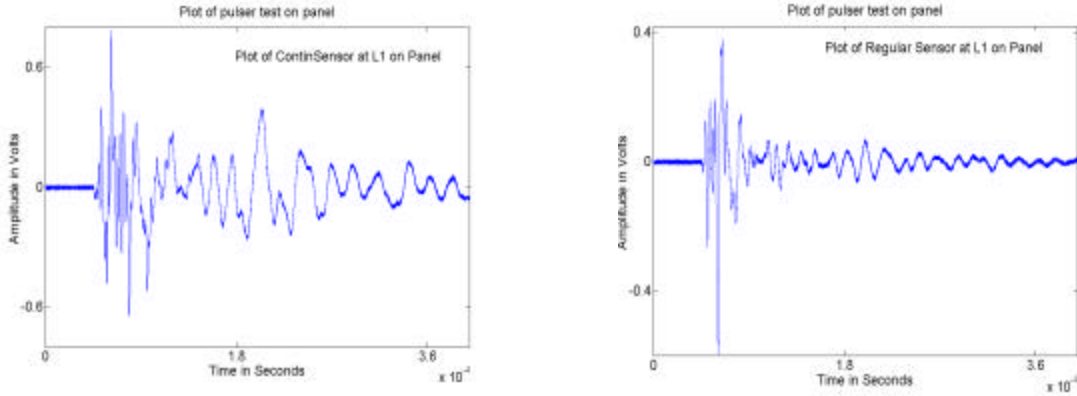**(a) Simulated AE events at location P_1**

Figure 9: comparison of responses from continuous sensor with single node sensor to simulated AE events at location P_1 (a) and (b) Continuous sensor; (c) and (d) single node sensor

The waveforms and wavelet maps corresponding to the continuous sensor as well as the single node sensor are shown in figure 9. For the simulated AE events from location P_1, the continuous sensor was found to have somewhat better sensitivity to higher frequency components of the simulated AE event, which may be partially attributed to the smaller source to sensor distance. Another important feature that is of interest is that the noise level in the continuous sensor was similar to that of the commercially available sensor in spite of the fact that the continuous sensor had six nodes and longer interconnecting cables. The some of the modal components of the signal from the continuous sensor lasted longer duration probably because of the modes successively hitting the individual sensor nodes. Figure 10 shows the comparison of similar responses when the pulser is moved to location P_2, which results in a longer source to sensor distance for the single node sensor at C_3. From a comparison of the waveforms, the signal from the continuous sensor was more than an order of magnitude stronger particularly in the high frequency

16

components and hence has far better signal to noise ratio compared to the single node sensor. It should be emphasized again that the signal amplitudes in the wavelet maps are normalized and hence do not reflect the true signal amplitudes.

The simulation illustrates the high level of attenuation present in composite panel compared to the aluminum plate particularly for the high frequency modes of the acoustic emission signals.   It also illustrates the advantage offered by the continuous sensor with distributed nodes for such situations.

(b) Pulser is at location 2.
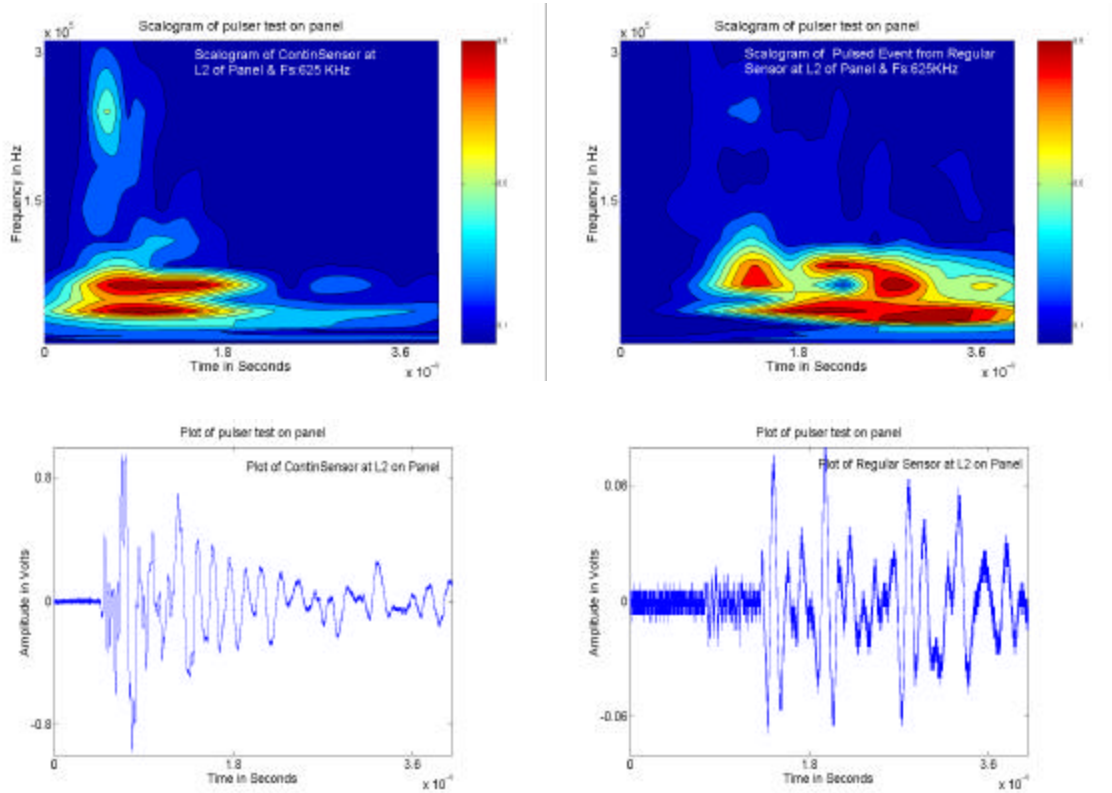
Figure 10: comparison of responses from continuous sensor with regular sensor at location P_2

6.0 Monitoring Acoustic Emission Signals from Incremental Fatigue Crack Growth

The panel was gripped between the loading plates shown in figure 11 and mounted on a 20 ton MTS testing machine. The load from the grips was introduced into the panel uniformly across the panel width through the gripping plates. To avoid any damage to the panel in the region over which the load was being introduced into the panel, relatively thick gripping plates and a total of twelve bolts were employed at each of the gripping regions. The bolts were tightened using a torque wrench so that the bolt tensions were equal in all bolts. This ensured that most of the load from the steel plates were transferred to the composite panel through friction along the interface between the steel plates and the composite panel, and the possibility of bolt bearing type of damage was minimized. Acoustic emission signals were collected for several fatigue load segments with different load amplitudes. During all of these segments the load remained tensile throughout each of the cycles, and the R ratio was approximately +0.1. At relatively low fatigue load amplitudes AE signals occurred intermittently and the signal amplitudes from the continuous sensor were 50 mV or smaller. As the fatigue load amplitude increased, the AE signal amplitudes also increased and they started to occur during each of the loading cycles. To ensure that the signals recorded were indeed from the fatigue crack growth and were not extraneous noise caused by the hydraulics of the testing machine or the fretting between the loading plates and composite panel, guard sensors were positioned near the gripping plate at locations C_1 and C_2 as shown in figure 8. A comparison of the time of arrival of the signals from the continuous sensor and the guard sensors indicated that the signals recorded by the continuous sensor were valid acoustic emission signals

originating from the two fatigue cracks at the center of the panel. After ascertaining the absence of extraneous noise, the single node sensors were moved from the locations C_1 and C_2 to locations C_3 and C_4 near the fatigue cracks so that these sensors are also are located at the proximity of the fatigue cracks. The signals that are described below were those that were collected during the largest cyclic load amplitudes.
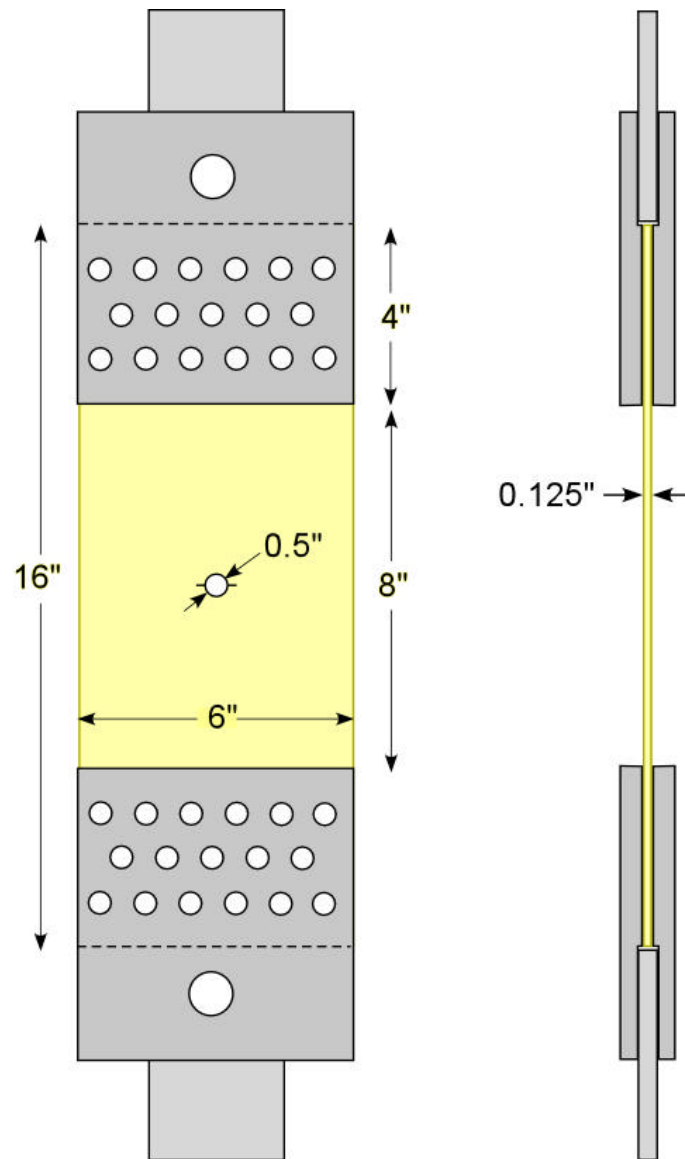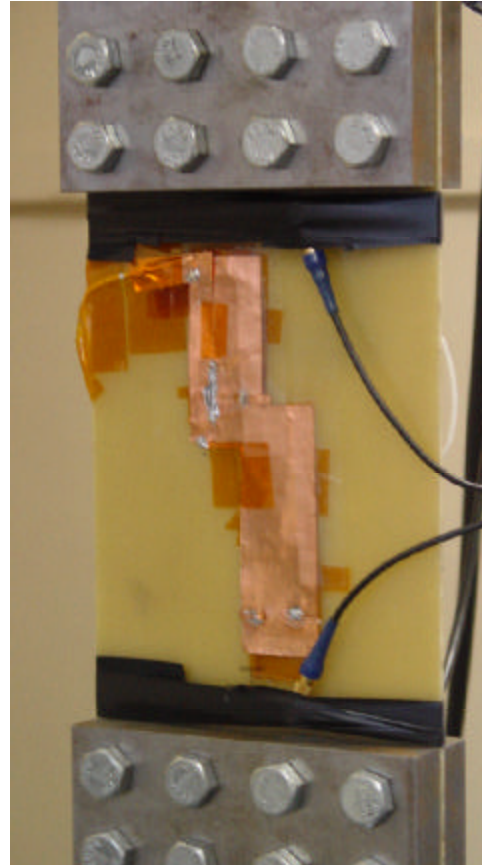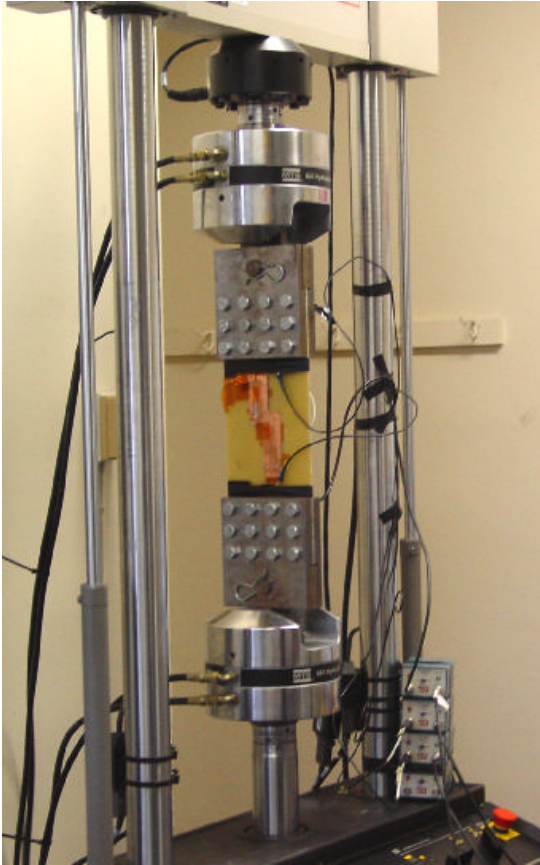
Figure 11. Composite panel with loading fixtures

Figure 12: The composite panel mounted in the MTS testing machine; (b) closeup view of the panel with the continuous sensor and the guard sensor.
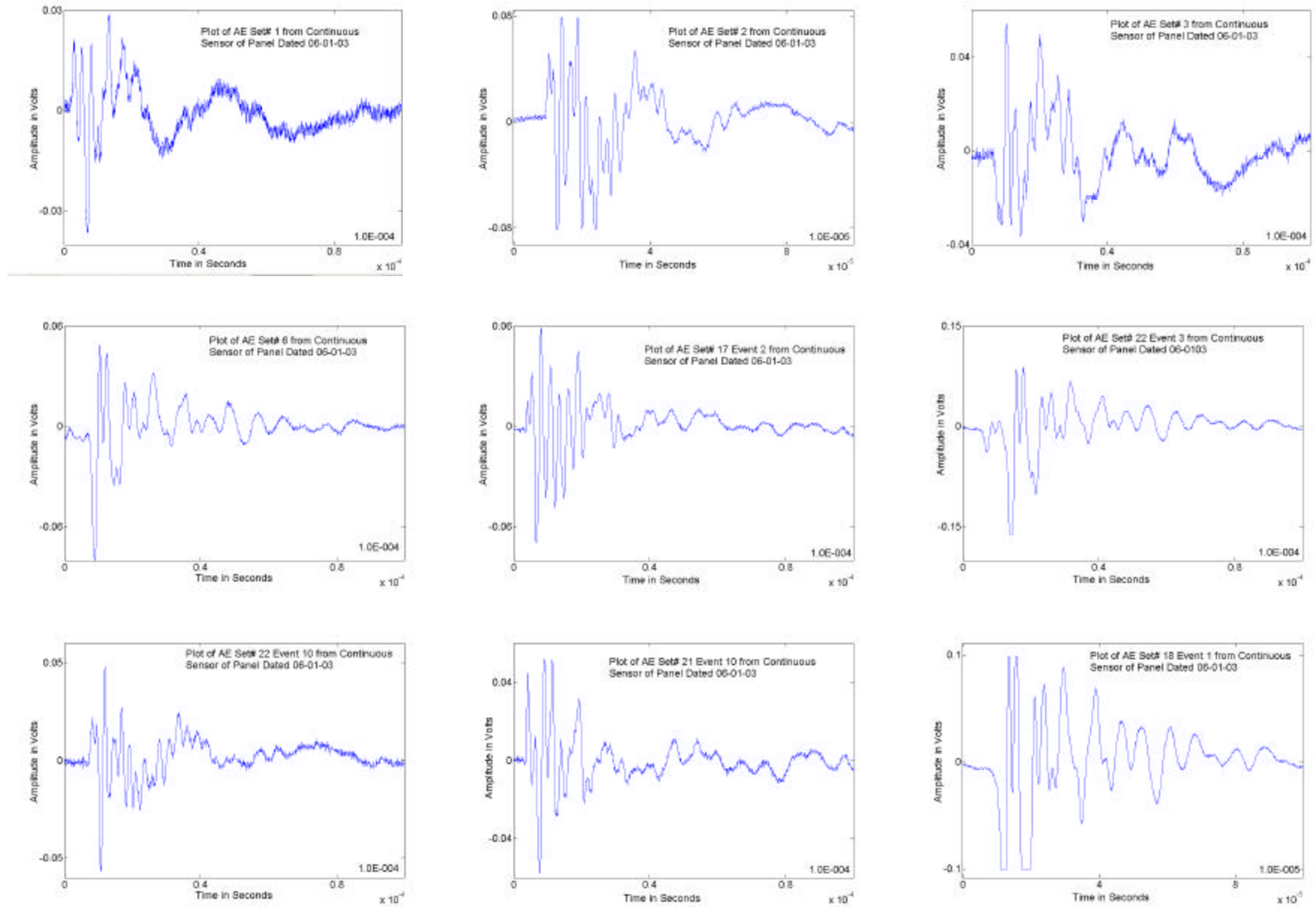
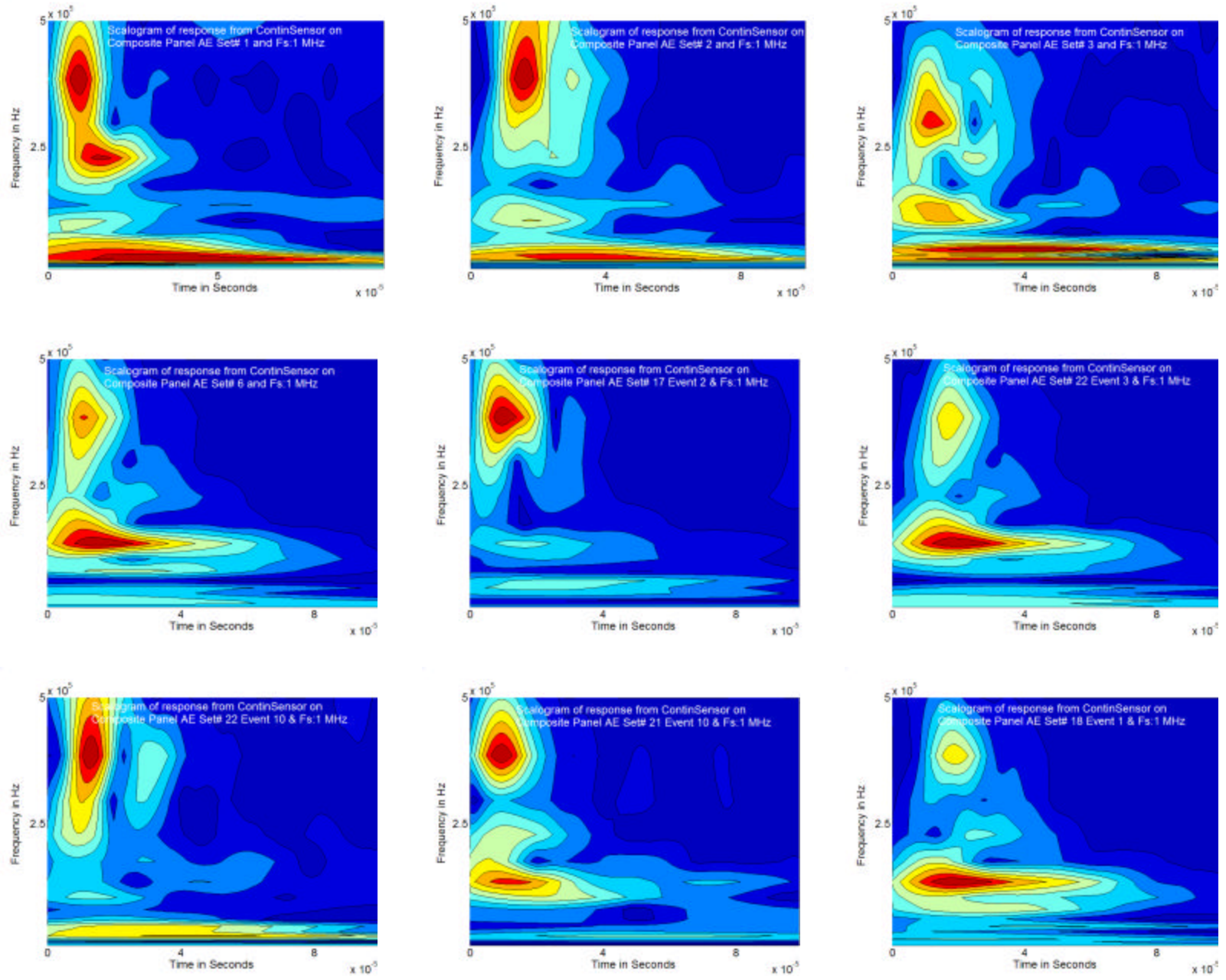Figure 13. Different types of acoustic emission signals received during the fatigue loading of the composite panel

Figure 14: The Morlet wavelet maps of the different types of the AE signals from continuous sensor

Several hundreds of acoustic emission signals from the continuous sensor as well as from the single node sensors were collected during fatigue cycles. Only the signals from the continuous sensor are described in this section. The cracks on either side of the circular hole grew approximately about 1.5 mm during this period. During this period all of the incremental crack extensions were expected to be mode I crack extensions and hence to be similar in nature. However, the source events, corresponding to the individual AE waveforms, could have had several differences. For example, there could be differences in the length of the instantaneous crack extensions or some of the material features such as local fiber volume fraction. Even though the waveforms looked similar there were minor differences among the shapes. Based on these shapes, nine representative waveforms were selected for inclusion in this report. These waveforms are shown in figure 13. The waveforms were originally recorded at sample rates of 10 million samples/second or greater. For performing the wavelet analysis, the signals were resampled at 1 million samples per second. Figures 14 show the corresponding wavelet maps for the nine types of AE signals. The differences among these signals are the relative magnitudes of the different frequency modes and the duration over which they are present.

7.0 Planar location of AE sources using continuous sensors

Earlier [2] continuous sensor was shown to successfully locate AE sources along a bar. This procedure is extended for location of AE sources in a plane. This work includes the development of the algorithm for locating the source using the single channel acoustic

emission signal from the continuous sensor. Illustrations of the numerical simulations are shown in this section. Figure 15 shows the typical AE signal after the signal has been processed to extract a Lamb wave mode suitable for location. Figure 15(b) shows the arrival times of the four such pulses used in the numerical simulation and the corresponding delta-t's. Knowing the locations of the individual nodes of the continuous sensor and the delta-t's, the algorithm locates the AE sources. Figure 16 shows the sensor node locations and a number of AE sources used in the numerical simulations.
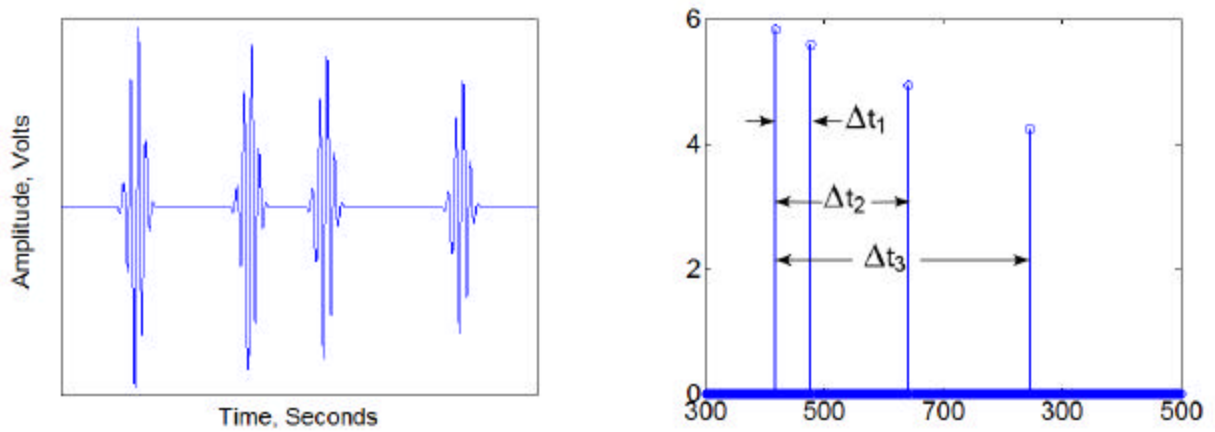

Figure 15: (a) Sketch illustrating a hypothetical AE signal from a continuous sensor monitoring a panel after signal processing to extract a suitable mode, (b) The delta-t's obtained in the numerical simulation of the source location algorithm for planar location.
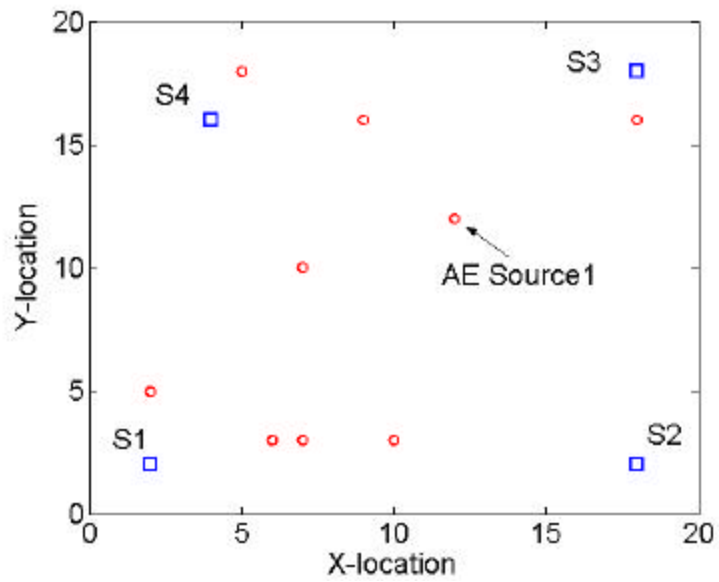
Figure 16: The nodes S_1 to S_4 (blue squares) of a four node continuous sensor and the AE sources (red circles) that were detected in the numerical simulation of AE sources

8.0 Development of the emulator for AE local processor

The Intelligent Structures and Mechanisms (ISM) Lab at NC A&T State University has patented a technique where piezoceramic (PZT) sensors are used to sense acoustic emissions (AE's) resulting from structural fatigue (e.g. cracking). Specifically, they have patented a continuous sensor array (CSA), capable of significantly reducing the complexity of SHM systems. A key element in this novel AE SHM system is a dedicated local processor chip, which acquires and processes AE signals. To prove the feasibility of this concept a prototype has been developed to emulate the acoustic emission processor (AEP). The AEP emulator will to be used for field-testing and verification of AE detection algorithms prior to developing a custom very large-scale integrated circuit (VLSI).
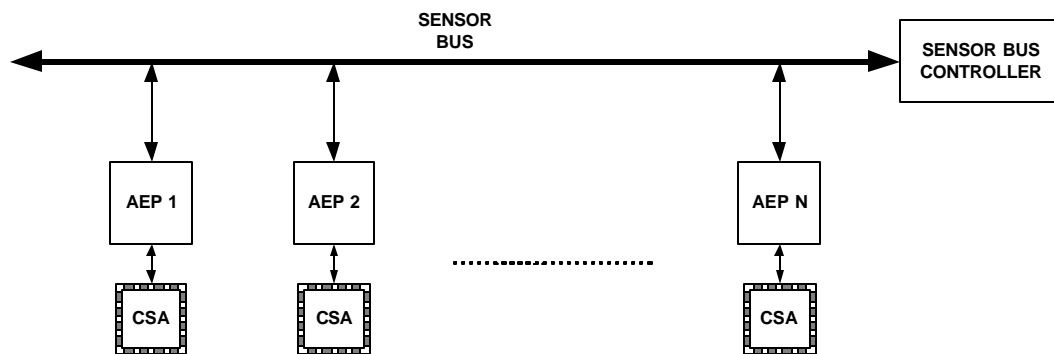

Figure 17: AE SHM system.

SHM systems will typically have several continuous sensor arrays (CSAs) interfaced to a single "sensor bus" which would be terminated with a sensor bus controller. This configuration results in the structure acquiring the equivalent of a central nervous system. A CSA can have up to 16 nodes connected in a series configuration.

Each CSA requires a dedicated AEP to acquire, process, and detect AE signals and interface to the digital sensor bus, as schematically shown in figure 17.

Emulator Description

A PC based simulator/emulator (using custom software and off-the-shelf data acquisition hardware) has been developed as a means to determine the viability of the AEP/CSA combination in a SHM system. A photograph of the system is displayed in Figure 18.
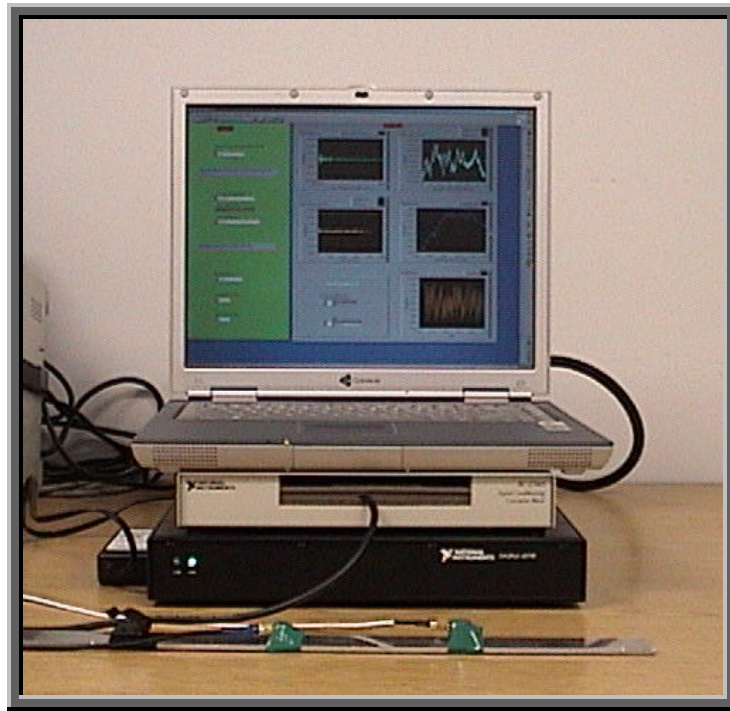

Figure 18: System for emulation of the AEP.

To minimize development time and simplify reprogramming, the software platform, "LabView" by National Instruments, has been used. Labview provides a graphical programming environment to facilitate the implementation of the AEP's signal

processing algorithms. In addition, LabView interfaces directly with the data acquisition hardware, which in this case, is a high-speed analog-to-digital converter (ADC) with custom external analog signal conditioning. Finally, the LabView based system allows algorithms to be easily and quickly be modified to accommodate unexpected conditions in the field.

Hardware Description

The hardware consists of a CSA, a signal conditioning gain stage "**G**", an anti-aliasing filter (AAF), an ADC, a PC (laptop) and the transducer bus interface module (TBIM). Figure 19 shows the signal flow through these blocks. The PC is responsible for emulating the function of the AEP.
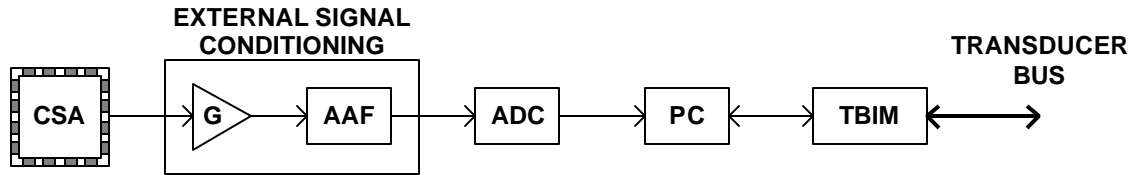

Figure 19: Signal flow through the AEP emulator.

Software description

The AEP soft model performs the tasks of acquiring data from the external ADC, processing/compressing the data, and formatting the data for transmission. Figure 20, the AEP soft model block diagram, contains all the functions necessary to implement the AEP.
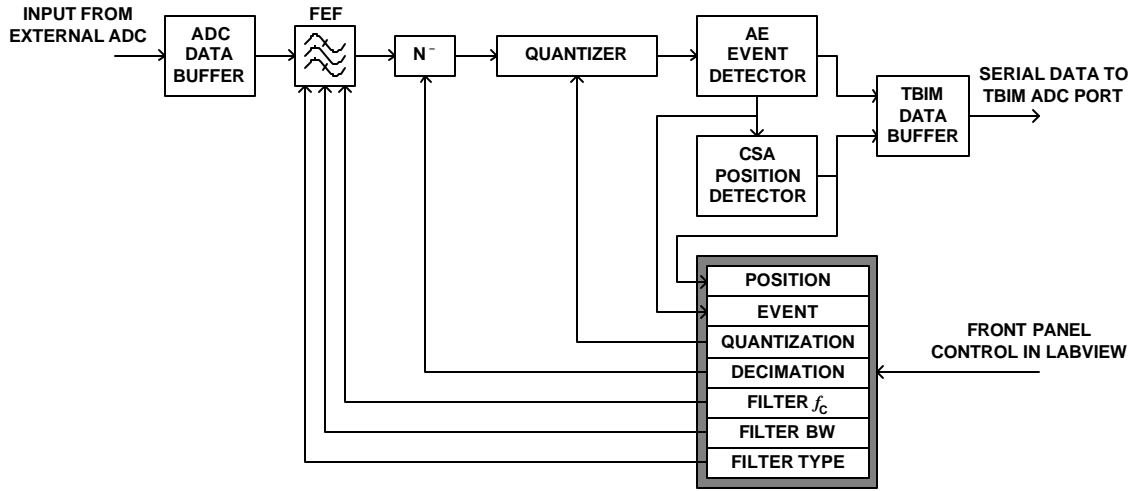
Figure 20: Soft model of AEP.

By virtue of the soft model implementation, access will be provided to critical parameters through the graphical front panel or software changes (see Figure 21). Hence, AEP algorithms can be optimized prior to committing to a custom VLSI realization.

Applications of prototype

The AEP emulator has been through initial testing in the lab and will be ready for field testing in two to three weeks. With its high degree of reconfigureability it will be suitable for any number of different SHM applications.
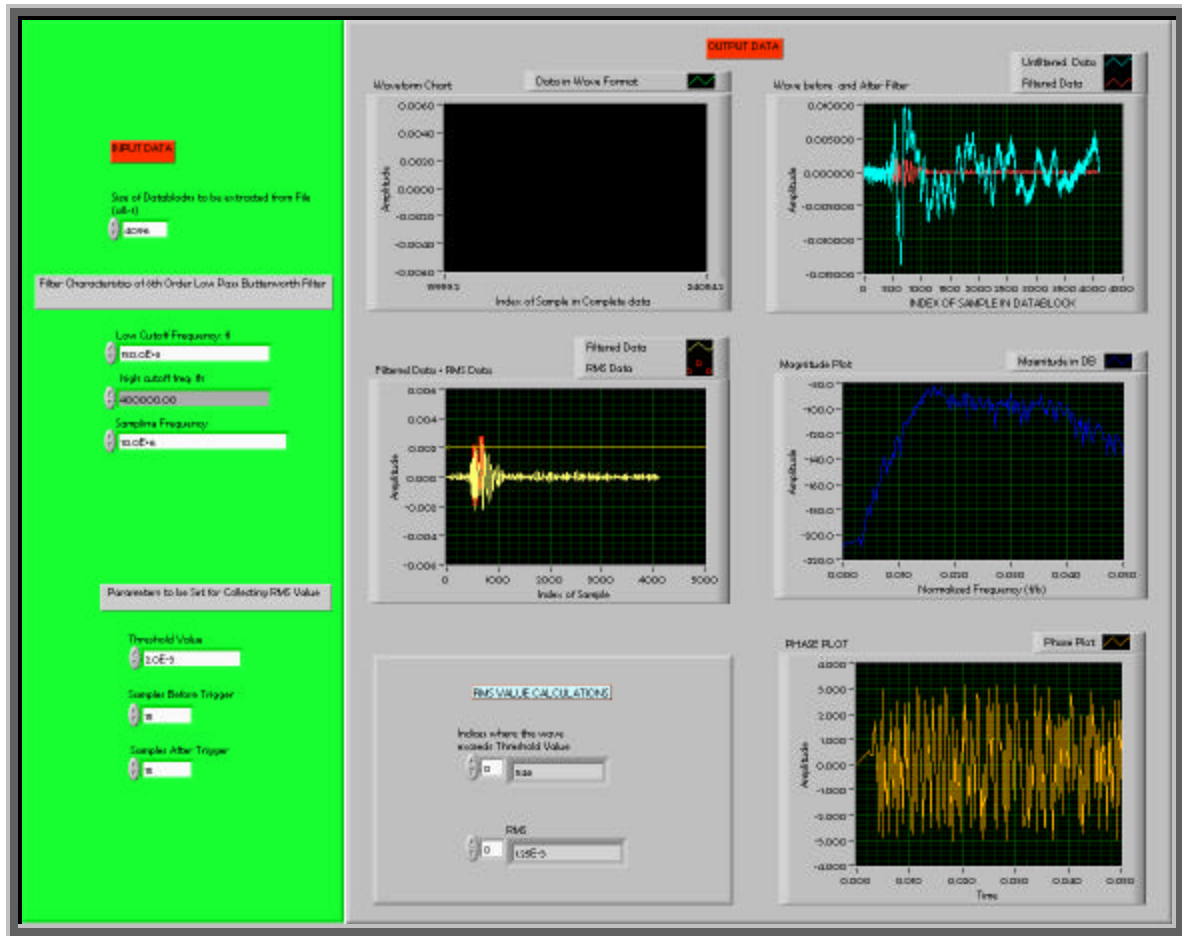
Figure 21: AEP emulator front panel.

Figure 22: AEP emulator in the lab.

9.0 Summary

The concept of Continuous Sensor is successfully applied to monitor crack extensions in a composite panel. Different types of acoustic emissions waveforms were seen. The continuous sensor has several advantages compared to conventional sensors in monitoring composite structures.

10.0 Acknowledgement

11.0 References

1. Sundaresan, M.J., Ghoshal, A., Schulz, M.J., "A Continuous Sensor to Measure Acoustic Waves in Plates," Journal of Intelligent Material Systems and Structures, Vol. 12, No.1, pp.41-56, January 2001.

2. Sundaresan, M.J., Schulz, M.J., Ghoshal, A., "Linear Location of Acoustic Emission Sources with a Single Channel Distributed Sensor," Journal of Intelligent Material Systems and Structures, Vol. 12, No. 10, pp.689-700, October 2001.

3. Sundaresan, M.J., Schulz, M.J., Ghoshal, A., and Martin, W.N., "A Neural System for Structural Health Monitoring," Proc. SPIE Vol. 4328, pp.130-141, 2001.